J|A|C|S COMMUNICATIONS

Published on Web 03/02/2009

# Control of Pore Size and Functionality in Isoreticular Zeolitic Imidazolate Frameworks and their Carbon Dioxide Selective Capture Properties

Rahul Banerjee, Hiroyasu Furukawa, David Britt, Carolyn Knobler, Michael O'Keeffe, and Omar M. Yaghi*

*Center for Reticular Chemistry, Department of Chemistry and Biochemistry, University of California—Los Angeles, 607 East Charles E. Young Drive, Los Angeles, California 90095*

Received December 3, 2008; E-mail: yaghi@chem.ucla.edu

Microporous materials such as zeolites are among the most important of inorganic materials, and extensive efforts have been devoted to their synthesis. A significant development in this regard was the introduction of organic structure-directing agents by R. M. Barrer and his co-workers almost 50 years ago.[1] However, despite the efforts of a large number of groups worldwide and the demonstration that at least millions of theoretical possibilities exist, less than 200 different structure types are known.[2,3] Indeed, it is probably fair to say that the mechanism by which structure-directing agents actually direct the formation of a particular structure is poorly understood, and efforts to design syntheses a priori have not been very successful. In contrast, the development, especially in the past decade, of metal—organic frameworks (MOFs), in which molecular building units are held together by strong bonds, has led to a new class of microporous materials (with some thousands of members) and to the development of a new discipline, *reticular chemistry*.[4] In this case, desired topologies can be achieved by design and, in particular, *isoreticular series* of compounds with the same topology but different sizes and functionalities of cavities can be prepared.[5]

A recent advance has been the development of a class of MOFs known as zeolitic imidazole frameworks (ZIFs), in which metal atoms such as Zn are linked through N atoms by ditopic imidazolate ($C_3N_2H_3^-$ = Im) or functionalized Im links to form neutral frameworks (Figure 1). These compounds have high chemical and thermal stabilities.[6] Although a few metal Im's have been known for decades,[7] the use of high-throughput methods and functionalized Im linkers has led to the preparation of a wide variety of structures that feature, significantly, zeolite (nine types) or zeolite-like (five types) frameworks.[8] However, just as for zeolites themselves, it now proves hard to target a definite topology, although some results can be rationalized in hindsight. Indeed, the topology appears to be determined by the specific functionalization of the imidazolate.[9] A further problem is that although ZIFs with giant pores have been discovered,[10] with one exception the windows in known ZIFs have rather small diameters. The exception is a Zn salt of a substituted imidazole with the gmelinite (zeolite code **GME**) topology.[2,8] This structure has wide channels formed by ~16 Å diameter rings of Zn—Im—Zn links. Clearly, it would be very desirable to produce materials with the **GME** topology and a wide range of pore metrics and functionalities for gas separations.

Here we describe a new method for achieving precisely controlled metrics and functionality in an isoreticular series of eight ZIFs with the desirable **GME** topology. Specifically, we report the synthesis and characterization of five new ZIFs, ZIF-78, -79, -80, -81, and -82, and three previously reported ZIFs,[8] ZIF-68, -69, and -70, and describe their exceptional ability to capture $CO_2$. Within this series, the pore diameter was varied incrementally from 7.1 to 15.9 Å and the Im link functionality altered from polar (—$NO_2$, ZIF-78; —CN, ZIF-82) to nonpolar (—$CH_3$, ZIF-79). We have found that ZIF-78 is the most effective $CO_2$ adsorbent and shows the highest selectivity for capture of $CO_2$ from binary mixtures with methane, nitrogen, and oxygen.

In earlier work, we observed that with 2-nitroimidazole (nIm) as the sole linker, the smaller-pore **SOD** topology (ZIF-65) resulted.

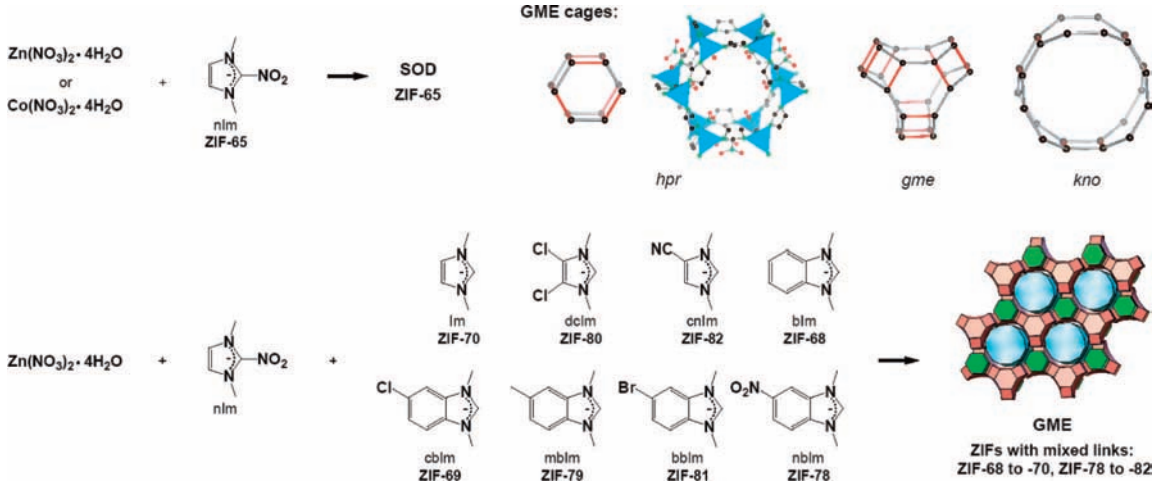


***Figure 1.*** Structures of imidazolate links and their abbreviations. Reaction of nIm results in the **SOD** topology. Reaction of nIm plus any other imidazole linker shown results in the **GME** topology, whose tiling is shown at the bottom right. The name of the ZIF resulting from reaction with nIm is given under each linker. At the top right are illustrated the *hpr*, *gme*, and *kno* cages, which make up the **GME** topology. Red edges indicate nIm linkers and gray edges substituted Im linkers. The chemical structure of the *hpr* cage is also shown. H atoms have been omitted for clarity. C, black; N, green; O, red; Zn, blue tetrahedra.

10.1021/ja809459e CCC: $40.75 

***Table 1.*** Chemical Composition of the **GME** ZIF Structures, Their Surface Areas ($A$), and the Pore Diameters ($d_p$) and Pore Apertures ($d_a$) of Their *kno* Cages

| ZIF-*n* | composition | elemental microanalysis (%)[a] | $A$ ($m^2/g$)[b] | $d_p$ (Å) | $d_a$ (Å) |
|---|---|---|---|---|---|
| ZIF-70 | $Zn(Im)_{1.13}(nIm)_{0.87}$ | C, 29.77 (29.93); H, 2.12 (2.14); N, 28.36 (28.34); Zn, 27.01 (27.16)[c] | 1730 | 15.9 | 13.1 |
| ZIF-80 | Zn(dcIm)(nIm) | –[d] | –[d] | 9.8 | 13.2 |
| ZIF-82 | Zn(cnIm)(nIm) | C, 31.09 (31.19); H, 1.51 (1.50); N, 31.76 (31.19); Zn, 24.51 (24.25) | 1300 | 12.3 | 8.1 |
| ZIF-68 | Zn(bIm)(nIm) | C, 40.09 (40.49); H, 2.12 (2.38); N, 23.60 (23.62); Zn, 21.95 (22.05)[c] | 1090 | 10.3 | 7.5 |
| ZIF-69 | Zn(cbIm)(nIm) | C, 35.90 (36.28); H, 1.81 (1.83); N, 20.76 (21.16); Zn, 19.51 (19.75)[c] | 950 | 7.8 | 4.4 |
| ZIF-79 | Zn(mbIm)(nIm) | C, 42.91 (42.81); H, 2.81 (2.95); N, 22.76 (22.70); Zn, 21.11 (21.18) | 810 | 7.5 | 4.0 |
| ZIF-81 | Zn(bbIm)(nIm) | C, 32.10 (32.16); H, 1.61 (1.62); N, 18.56 (18.16); Zn, 17.51 (17.50) | 760 | 7.4 | 3.9 |
| ZIF-78 | Zn(nbIm)(nIm) | C, 35.30 (35.37); H, 1.81 (1.78); N, 24.76 (24.75); Zn, 19.61 (19.25) | 620 | 7.1 | 3.8 |

[a] For activated samples; calculated values shown in parentheses. [b] Calculated by the BET method. [c] First reported in the Supporting Online Material for ref 8. [d] ZIF-80 was not scaled up.

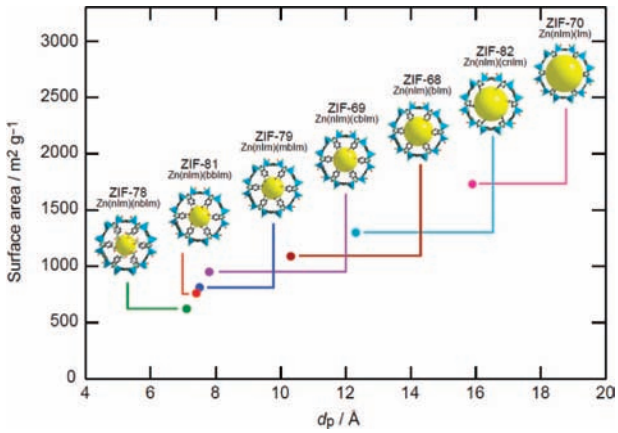


***Figure 2.*** Plot of pore diameter ($d_p$) vs surface area for the **GME** ZIFs, indicating a nearly linear relationship. To illustrate the variation of the pore size and functionality, the *kno* cage of each ZIF is shown. H atoms have been omitted for clarity. C, black; N, green; O, red; Cl, pink; Br, brown; Zn, blue tetrahedra.

Remarkably, however, the **GME** topology (ZIF-68 to -70) was obtained when two distinct linkers, one of which had to be nIm, were simultaneously employed (Figure 1, bottom).[8] Following this lead, we successfully prepared a range of **GME** ZIFs using equimolar amounts of nIm and a second substituted Im. The second link is the key to achieving a wide range of pore diameters and functionalities.

The ZIFs reported here were synthesized solvothermally in a high-throughput fashion and scaled up to multigram quantities.[11,12] The structures of ZIF-78 to -82, were determined from single-crystal X-ray diffraction data.[12,13] Those of ZIF-68 to -70 were reported earlier.[8] In each ZIF, every tetrahedral Zn atom is connected to two nIm and two other substituted Im. The tetrahedra are linked by corner sharing into three-dimensional frameworks with the **GME** topology, wherein the Si and O atoms of **GME** zeolite are replaced with Zn(II) and Im-type links, respectively. As illustrated in Figure 1, the structure can be described as being built from *kno* [$4^3.8^3.12^2$] cages (24 Zn ions) forming channels of 12-membered rings parallel to the *c* axis, cross-linked by *gme* [$4^9.6^2.8^3$] cages (18 Zn ions) and *hpr* [$4^6.6^2$] cages (12 Zn ions) in the ratio 1:1:1 (the symbol [...$m^n$...] indicates that $n$ faces of the cage are $m$-membered rings). In the GME framework, there are four crystallographically distinct links. Interestingly, the nIm links always occupy the same two edges, which are part of the *hpr* cages, and the other substituted Im's occupy the remaining edges (Figure 1). Across the series of Im linkers with −Cl, −CN, −Me, −Br, and $-NO_2$ functionality incorporated into the **GME** topology, the substituted Im's point into the voids of the *kno* cages. Thus, by varying the substituted Im, one can systematically modulate the pore aperture of the *kno* cage from 3.8 to 13.1 Å and the pore diameter from 7.1 to 15.9 Å (see Table 1).[14] The flexibility with which the pores can be controllably adjusted while maintaining the underlying topology makes these ZIFs highly attractive for many studies, including gas separations.

To evaluate the porosities of these ZIFs, we first examined their thermal stabilities using thermal gravimetric analysis (TGA) of the as-synthesized, solvent-exchanged, activated samples.[12] The TGA curves demonstrated the high thermal stabilities of the ZIFs. TGA traces for the as-synthesized and methanol-exchanged ZIFs showed a long plateau in the temperature range 150−390 °C, similar to that for the previously reported ZIFs (ZIF-68 to -70). The plateau regions were also observed in the activated samples, which is indicative of thermal stability even in the absence of guest molecules. The thermal stabilities of ZIF-78, -79, -81, and -82 were further confirmed by the coincidence of the powder X-ray diffraction (PXRD) patterns with those simulated from the single-crystal structures after heating to 300 °C under an $N_2$ atmosphere. Examination of chemical stability was performed by heating the as-synthesized samples in boiling benzene, methanol, and water for 7 days. Remarkably, all of the ZIFs retained their structures under these conditions, as evidenced by the sharp, unshifted diffraction lines in their PXRD patterns.[12]

Permanent porosity of the ZIFs was demonstrated by measuring the $N_2$ gas adsorption of the guest-free material. $N_2$ adsorption in these ZIFs exhibits the typical type-I isotherm, which indicates the microporosity of activated materials. The Brunauer−Emmet−Teller (BET) surface areas for the seven ZIFs vary from 620 to 1730 $m^2$ $g^{-1}$ (Table 1). The surface-area variation for these ZIFs alone is much wider than that for any other zeolite materials reported to date.[15] Furthermore, Figure 2 shows a nearly linear relationship between pore diameter and the specific surface area. This effect is likely the result of both reduced pore volume in the ZIFs with smaller pore dimensions and increased framework weight in the ZIFs bearing additional functional groups.

$CO_2$ uptake in MOFs is of great interest because of the need for effective $CO_2$ capture.[16] $CO_2$ uptake by the ZIFs was measured and compared with that by BPL carbon, which is currently widely used in industry for gas separations.[17] The $CO_2$ uptake values at 1 bar varied widely (Figure 3A), in the sequence $-NO_2$ (ZIF-78) > −CN, −Br, −Cl (ZIF-82, -81, -69) > $-C_6H_6$, −Me (ZIF-68, -79) > −H (ZIF-70) > BPL carbon. This order is in agreement with the greater attraction expected between the polar functional groups in the ZIFs and $CO_2$, which has a significant quadrupole moment. ZIF-78 takes up 3 times as much $CO_2$ as BPL carbon and outperforms the other ZIFs as well.[8−10] However, there is no noticeable relationship between $CO_2$ uptake and pore diameter. This result implies that $CO_2$ uptake capacity is influenced primarily by functionality effects rather than pore metrics. Therefore, we recorded $CH_4$, $N_2$, and $O_2$ isotherms for the ZIFs to further probe the effect of functionality on their gas-separation properties.

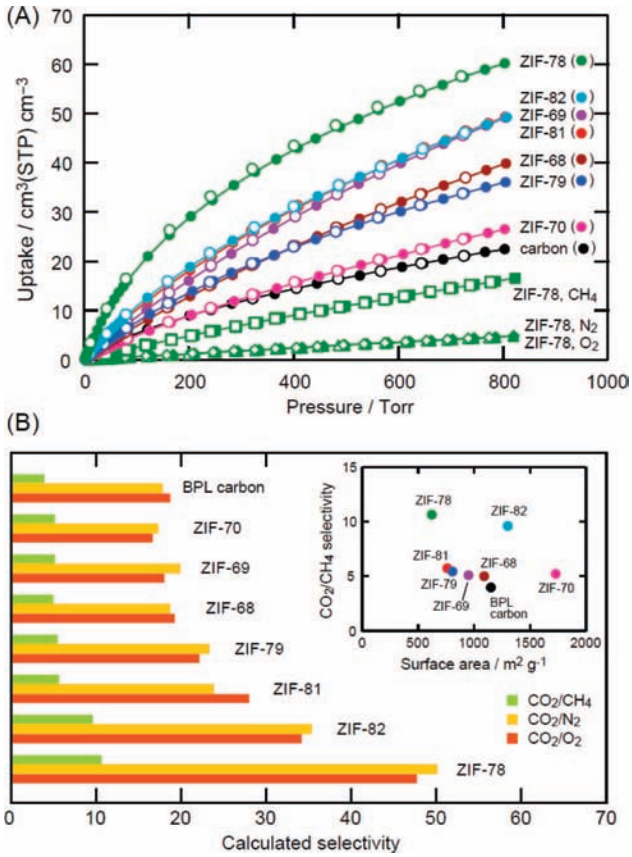


***Figure 3.*** (A) $CO_2$ isotherms of the **GME** ZIFs (excluding ZIF-80) and BPL carbon at 298 K. $CH_4$, $N_2$, and $O_2$ isotherms for ZIF-78 are also shown. Filled and open symbols represent adsorption and desorption branches, respectively. (B) Calculated $CO_2/CH_4$, $CO_2/N_2$, and $CO_2/O_2$ selectivities. (Inset) Surface-area dependence of the calculated $CO_2/CH_4$ selectivities.

As shown in Figure 3A, ZIF-78 has a higher affinity and capacity for $CO_2$ than for other gases. The $CO_2$ uptake at 800 Torr and 298 K for ZIF-78 is 4 times higher than the $CH_4$ uptake and 8−10 times higher than for $O_2$ and $N_2$. On the basis of the $CO_2$, $CH_4$, $N_2$, and $O_2$ isotherms measured at 273, 283, and 298 K, initial slopes of adsorption isotherms were estimated and then used to estimate the $CO_2/CH_4$, $CO_2/N_2$, and $CO_2/O_2$ selectivities (as ratios of the initial slopes). Figure 3B demonstrates that ZIF-78 and -82 have higher selectivities than the other ZIFs and BPL carbon. Since the $-NO_2$ and −CN groups in ZIF-78 and -82, respectively, have greater dipole moments than the other functionalities,[18] dipole−quadrupole interactions with $CO_2$ can be expected, as observed between supercritical $CO_2$ and organics in the past.[19] Thus, we conclude that interactions between $CO_2$ and these functionalities enhance the initial slopes of the $CO_2$ isotherms for ZIF-78 and -82, resulting in their greater selectivities.

The validity of calculated selectivities was confirmed by dynamic breakthrough experiments, which were performed according to known procedures.[20] In the case of 1%, 5%, and 20% $CO_2$ in a balance of $CH_4$, retention of $CO_2$ by ZIF-78, ZIF-82, and BPL carbon was observed. Longer retention of $CO_2$ was observed in the ZIF materials than in BPL carbon. Efficient removal of $CO_2$ would result in reduced emissions and substantially diminish the cost of natural gas production.[21] The highly selective $CO_2$ uptake in ZIFs, especially those having polar functionalities, indicates that they have potential to emerge as important materials for natural gas purification and landfill gas separation. Present work in our laboratory is focused on extending these studies to include *isoreticular functionalization* of other ZIFs[22] for preventing post-combustion $CO_2$ from reaching the atmosphere.

**Acknowledgment.** We thank BASF (Ludwigshafen, Germany) and DOE (DEFG0206ER15813) for funding.

**Supporting Information Available:** Detailed experimental procedures and data. This material is available free of charge via the Internet at http://pubs.acs.org.

## References

(1) Jansen, J. C. In *Introduction to Zeolite Science and Practice*; van Bekkum, A., Jacobs, P. A., Flanigen, E. M., Jansen, J. C., Eds.; Elsevier: Amsterdam, 2001.
(2) Baerlocher, C.; Meier, W. M.; Olson, D. H. *Atlas of Zeolite Framework Types*; Elsevier: Amsterdam, 2001.
(3) Delgado-Friedrichs, O.; Foster, M. D.; O'Keeffe, M.; Proserpio, D. M.; Treacy, M. M. J.; Yaghi, O. M. *J. Solid State Chem.* **2005**, *178*, 2533.
(4) Yaghi, O. M.; O'Keeffe, M.; Ockwig, N. W.; Chae, H. K.; Eddaoudi, M.; Kim, J. *Nature* **2003**, *423*, 705.
(5) Eddaoudi, M.; Kim, J.; Rosi, N.; Vodak, D.; Wachter, J.; O'Keeffe, M.; Yaghi, O. M. *Science* **2002**, *295*, 469.
(6) Park, K. S.; Zheng, N.; Côté, A. P.; Choi, J. Y.; Huang, R.; Uribe-Romo, F. J.; Chae, H. K.; O'Keeffe, M.; Yaghi, O. M. *Proc. Natl. Acad. Sci. U.S.A.* **2006**, *103*, 10186.
(7) Huang, X.-C.; Lin, Y.-Y.; Zhang, J.-P.; Chen, X.-M. *Angew. Chem., Int. Ed.* **2006**, *45*, 1557.
(8) Banerjee, R.; Phan, A.; Wang, B.; Knobler, C.; Furukawa, H.; O'Keeffe, M.; Yaghi, O. M. *Science* **2008**, *319*, 939.
(9) Hayashi, H.; Côté, A. P.; Furukawa, H.; O'Keeffe, M.; Yaghi, O. M. *Nat. Mater.* **2007**, *6*, 501.
(10) Wang, B.; Côté, A. P.; Furukawa, H.; O'Keeffe, M.; Yaghi, O. M. *Nature* **2008**, *453*, 207.
(11) Yields obtained for ZIF-68, -69, -70, -78, -79, -81, and -82 were 24, 33, 30, 28, 14, 26, and 24%, respectively. We note that these yields are unoptimized, and as with other MOFs and ZIFs, we expect that higher-yield conditions can be found. In a typical high-throughput synthesis, stock solutions of nIm (120 $\mu$L, 0.20 M), nbIm (120 $\mu$L, 0.20 M), and $Zn(NO_3)_2 \cdot 4H_2O$ (60 $\mu$L, 0.15 M) in *N*,*N*-dimethylformamide (DMF) were dispensed by a Gilson model 215 programmed liquid handler into a 96-well glass plate, which was sealed and heated to 100 °C for 96 h. In a typical bulk-scale synthesis, stock solutions of nIm (5 mL, 0.20 M), nbIm (5 mL, 0.20 M), and $Zn(NO_3)_2 \cdot 4H_2O$ (4 mL, 0.20 M) in DMF were mixed in a 10 mL glass vial, which was sealed and heated to 100 °C for 96 h. The mother liquor was then decanted and the precipitate washed three times with DMF. Yellow crystals of ZIF-78 were collected by filtration and dried in air for 10 min.
(12) See the Supporting Information for full experimental details.
(13) All of these ZIFs are hexagonal ($P6_3/mmc$). **ZIF-78**: $a = b = 26.1174(3)$ Å, $c = 19.4910(4)$ Å; $V = 11514.0(3)$ Å$^3$; total reflections (tr), 32033; independent reflections (ir), 1471; R1 = 0.0901, wR2 = 0.2607. **ZIF-79**: $a = b = 26.9263(3)$ Å, $c = 19.6532(4)$ Å; $V = 11440.5(3)$ Å$^3$; tr, 29358; ir, 1263; R1 = 0.0867, wR2 = 0.2671. **ZIF-80**: $a = b = 26.3070(4)$ Å, $c = 19.361(1)$ Å; $V = 11604.0(3)$ Å$^3$; tr, 16661; ir, 999; R1 = 0.0869, wR2 = 0.2796. **ZIF-81**: $a = b = 25.9929(12)$ Å, $c = 19.6997(19)$ Å; $V = 11526.6(13)$ Å$^3$; tr, 35687; ir, 1434; R1 = 0.0881, wR2 = 0.2225. **ZIF-82**: $a = b = 26.4422(3)$ Å, $c = 18.9703(4)$ Å; $V = 11486.8(3)$ Å$^3$; tr, 41682; ir, 2948; R1 = 0.0837, wR2 = 0.2798. Crystallographic data for the structures reported in this paper have been deposited with the Cambridge Crystallographic Data Centre)CCDC) under reference numbers 704995 to 705002. These data can be obtained free of charge at www.ccdc.cam.ac.uk/conts/retrieving.html or from the CCDC, 12 Union Road, Cambridge CB2 1EZ, U.K.
(14) All of the calculations were done using Cerius2 software (version 4.2, Accelrys); van der Waals radii were taken into consideration in all cases (C, 1.70; H, 1.20; O, 1.52; N, 1.55; Cl, 1.79; Br, 1.89 Å).
(15) Rouquerol, F.; Rouquerol, J.; Sing, K. *Adsorption by Powders & Porous Solids*; Academic Press: London, 1999.
(16) (a) Llewellyn, P. L.; Bourrelly, S.; Serre, C.; Vimont, A.; Daturi, M.; Hamon, L.; Weireld, G. D.; Chang, J.-S.; Hong, D.-Y.; Hwang, Y. K.; Jhung, S. H.; Férey, G. *Langmuir* **2008**, *24*, 7245. (b) Kitaura, R.; Seki, K.; Akiyama, G.; Kitagawa, S. *Angew. Chem., Int. Ed.* **2003**, *42*, 428. (c) Chen, B.; Ma, S.; Zapata, F.; Fronczek, F. R.; Lobkovsky, E. B.; Zhou, H.-C. *Inorg. Chem.* **2007**, *46*, 1233.
(17) Sircar, S.; Golden, T. C.; Rao, M. B. *Carbon* **1996**, *34*, 1.
(18) *CRC Handbook of Chemistry and Physics*, 74th ed.; Lide, D. R., Frederiksen, H. P. R., Eds.; CRC Press: Boca Raton, FL, 1993.
(19) Beckman, E. J. *Chem. Commun.* **2004**, 1885.
(20) Britt, D.; Tranchemontagne, D.; Yaghi, O. M. *Proc. Natl. Acad. Sci. U.S.A.* **2008**, *105*, 11623.
(21) Sircar, S. *Ind. Eng. Chem. Res.* **2006**, *45*, 5435.
(22) Morris, W.; Doonan, C. J.; Furukawa, H.; Banerjee, R.; Yaghi, O. M. *J. Am. Chem. Soc.* **2008**, *130*, 12626.

JA809459E